

High-Pressure Irreversible Amorphization of $\text{La}_{1/3}\text{NbO}_3$

Itzhak Halevy^{1,2}, Amir Hen³, Amir Broide¹, Mike L. Winterrose², Shimon Zalkind¹, Zhiqiang Chen⁴

¹Nuclear Research Center - Negev, Beer-Sheva, Israel

²Department of Materials Science, California Institute of Technology, Pasadena, USA

³Department of Nuclear Engineering, Ben Gurion University, Beer-Sheva, Israel

⁴NSLS, Brookhaven National Laboratory, New York, USA

E-mail: ihalevy@caltech.edu

Received February 5, 2011; revised March 28, 2011; accepted April 17, 2011

Abstract

The crystallographic structure of $\text{La}_{1/3}\text{NbO}_3$ perovskite was studied at high pressures using a diamond-anvil cell and synchrotron radiation. High-pressure energy dispersive (EDS) X-ray diffraction and high-pressure angle dispersive (ADS) X-ray diffraction revealed an irreversible amorphization at ~ 10 GPa. A large change in the bulk modulus accompanied the high-pressure amorphization.

Keywords: $\text{La}_{1/3}\text{NbO}_3$, High-Pressure, Amorphization, Perovskites

1. Introduction

The ABO_3 perovskites contain display a large variety of special properties such as ionic conductivity [1,2], magnetism [3] and ferroelectricity [4]. The A-site deficient ABO_3 compounds $\text{La}_{2/3-x}\text{Li}_x\text{TiO}$ [5,6] and $\text{La}_x\text{Li}_y\text{NbO}_3$ [7,8] have demonstrated high lithium ionic conductivity, which has the potential to be used as an electrolyte for the solid state lithium batteries and electrochromic devices. Due to the vacancies in their structure, it is favorable to use them as lithium intercalation hosts. The materials with intercalation capability are under consideration for use as electrode materials for the lithium ion battery. Inaguma et al. first reported the intercalation of lithium into $\text{La}_{0.51}\text{Li}_{0.34}\text{TiO}_{2.94}$ [1]. Recently, $\text{LiLaNb}_2\text{O}_7$ perovskite demonstrated an intercalation capacity of one lithium per formula [9].

The existence of a two-dimensional channel or three-dimensional tunnel in the structure of a compound with vacancies allows the lithium ions to be reversibly inserted into and extracted from its structure. Ideally, the metal ion in the compound should be multivalent, so that it can accept or donate electrons. The $\text{La}_{1/3}\text{NbO}_3$ perovskite meets these conditions. The perovskite to postperovskite phase has been investigated extensively, this despite that fact that it is difficult to quench at ambient pressure.

In this paper, the crystallographic structure and unit cell parameters of $\text{La}_{1/3}\text{NbO}_3$ were investigated under high pressure. A Rietveld analysis of the X-ray diffraction revealed an irreversible amorphization of $\text{La}_{1/3}\text{NbO}_3$

brought on by the application of pressure.

2. Experimental

2.1. Sample Preparation and Methods

The $\text{La}_{1/3}\text{NbO}_3$ perovskite was prepared from La_2O_3 and Nb_2O_5 (99.9%, Aldrich).

In order to improve the ordering of La^{3+} ions and the vacancies in $\text{La}_{1/3}\text{NbO}_3$ perovskite, the sample was then heated at 800°C for 3 days and quenched in liquid nitrogen.

The sample was checked for the morphology and impurities by a JEOL SEM (Scanning Electron Microscope).

2.2. Diamond Anvil Cell (DAC)

Pressure (up to 36.4 GPa) was generated using a "Tel-Aviv"-type diamond anvil cell (DAC) (a type of Merrill-Bassett DAC) [11]. The experiments were conducted using a monochromatic and polychromatic X-ray beam. The high pressure measurements were carried out on a sample ~ 30 μm in thickness and 100 μm in diameter. The pressure was measured using the Ruby fluorescence technique [12].

Ethanol methanol (4:1) in the sample cavity was used as a pressure medium. The pressure distribution inside the sampling space was checked at different regions, and was determined to vary by less than 5%.

Data was acquired for approximately 15 - 30 minutes at each pressure step.

2.3. Ambient Pressure X-Ray - ADS

The XRD patterns were taken with a Phillips PW1730 diffractometer with Cu-K α radiation and SiO₂ monochromator. The powder was grounded carefully to a micron grain size.

The measurement of the La_{1/3}NbO₃ perovskite was taken in the range of 10° - 120° with a speed of 5 sec/step.

2.4. High-Pressure X-Ray - EDS

High-pressure Energy dispersive (EDS) X-ray diffraction studies were performed at beamline X17-C of the National Synchrotron Light Source (NSLS) (**Figure 1**, bottom). The energy dispersive data were collected using a HPGe detector with the energy region 0 - 80 KeV. The high-pressure X-ray powder-diffraction measurements were taken at discrete pressure steps in the range of 0 GPa to 34.7 GPa. The data was collected by the energy-dispersive (EDS) technique using polychromatic X-ray beam focused with KB mirrors. The energy dispersive measurements were carried out in transmission configuration using a 100 μ m collimator and energy spectrum detector technique. The data was analyzed using a commercial Rietveld analysis software package [13]. The energy data was converted to the 2 θ dimension as with a CuK α_1 radiation ($\lambda = 1.5406 \text{ \AA}$).

2.5. High-Pressure X-Ray - ADS

High-pressure angle dispersive (ADS) X-ray diffraction studies were performed at beamline X17-C of the National Synchrotron Light Source (NSLS) (**Figure 1**, up). A sagittally bent Si Laue crystal monochromator was used with a KB focusing mirror.

The angle dispersive data were collected using a 2D detector, Rayonix SX-165 CCD, with opening Bragg angle ($2\theta = 30^\circ$). The high-pressure X-ray powder-diffraction measurements were taken at discrete pressure steps in the range of 0 to 34.0 GPa. The data was collected by the angle-dispersive (ADS) technique. A monochromatic X-ray beam ($\lambda = 0.4066 \text{ \AA}$) from the high-order Si crystal monochromator was used. The angle dispersive measurements were carried out in transmission configuration using the 2D image detector technique. The data was analyzed using a commercial Rietveld analysis software package [13]. The 2D data was converted to the 2 θ dimension by the Fit2D [14] software.

3. Results and Discussion

The sample was checked for morphology and impurities using a JEOL SEM (scanning electron microscope). The

morphology micrograph of the La_{1/3}NbO₃ is depicted in **Figure 2**, at a magnification of $\times 200$ and an insert of $\times 1000$.



Figure 1. Beamline X17-C of the National Synchrotron Light Source (NSLS). High-pressure energy dispersive (EDS) *bottom* and high-pressure angle dispersive (ADS) *up*.

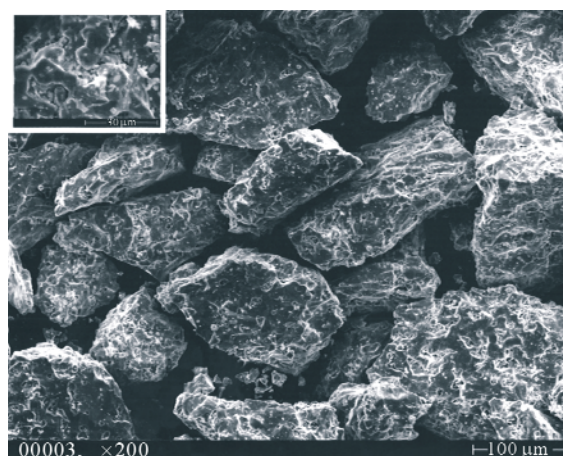


Figure 2. Morphology micrograph of the La_{1/3}NbO₃, measured by a JEOL SEM (scanning electron microscope) at a magnification of $\times 200$ and an insert of $\times 1000$. Using the EDS technique the stoichiometric ratio was confirmed. There was no detectable evidence of impurities in the sample.

Ambient X-ray diffraction measurements were carried out to confirm the initial crystallographic structure. The diffraction pattern obtained using $\text{CuK}\alpha$ radiation ($\lambda = 1.5406 \text{ \AA}$) is shown in **Figure 3**.

The diffraction details are; $2\theta = 9^\circ - 140^\circ$, $\Delta 2\theta = 0.02^\circ$, 10 sec/channel, 40 kV and 35 mA.

The data was analyzed with Rietveld analysis to the Cmmm symmetry. The GOF [13] (goodness of fitness) is 5.59%. In this case the fitting to Pmmm symmetry is very comparable but with a higher GOF of 8.9%. We confirm the structure to be Cmmm as was found by Kennedy [10]. The unit cell parameters that were derived are $a = 7.8422(2) \text{ \AA}$, $b = 7.8220(2) \text{ \AA}$ and $c = 7.9147(2) \text{ \AA}$. It looks like a and b are a bit lower while c is a bit higher compared to Kennedy's results. This discrepancy might be due to different sample preparation methods.

The $\text{La}_{1/3}\text{NbO}_3$ was loaded into the diamond anvil cell with ethanol methanol (4:1) and ruby for ADS X-ray diffraction. In **Figure 4**, we see the X-ray diffraction patterns at discrete pressure steps. In the center of the picture, we can see the beam stop and the beam stop holder that protect the detector from the main beam. In the two first pictures we see the Debye circles which are a bit

grainy, indicating a crystalline phase with large grain size. Qualitatively, we see at a pressure of 12.5 GPa that the crystalline lines are fading and wide ring has appeared, indicating that the amorphous state is appearing.

The amorphous state holds to the highest pressures examined (33.1 GPa). On releasing the high pressure the amorphous state persisted down to ambient pressure. We thus clearly observe an irreversible amorphization of $\text{La}_{1/3}\text{NbO}_3$ at high pressures.

This initial result led to two more sets of measurements on $\text{La}_{1/3}\text{NbO}_3$, employing the ADS and EDS techniques.

The ADS data of $\text{La}_{1/3}\text{NbO}_3$ (**Figure 5**) was collected with higher detector resolution (Rayonix SX-165 CCD) and with smaller pressure steps. This facilitates separate analysis of the crystalline and amorphous phases. **Figure 5** clearly shows that the structure starts in a crystalline state (Cmmm) and transitions to an amorphous state as the pressure is increased. Between 9.5 GPa to 12 GPa we found a superposition of the two states, likely due to a finite transition region and perhaps to pressures gradients in the diamond anvil cell.

Rietveld analysis on the crystalline state gave the

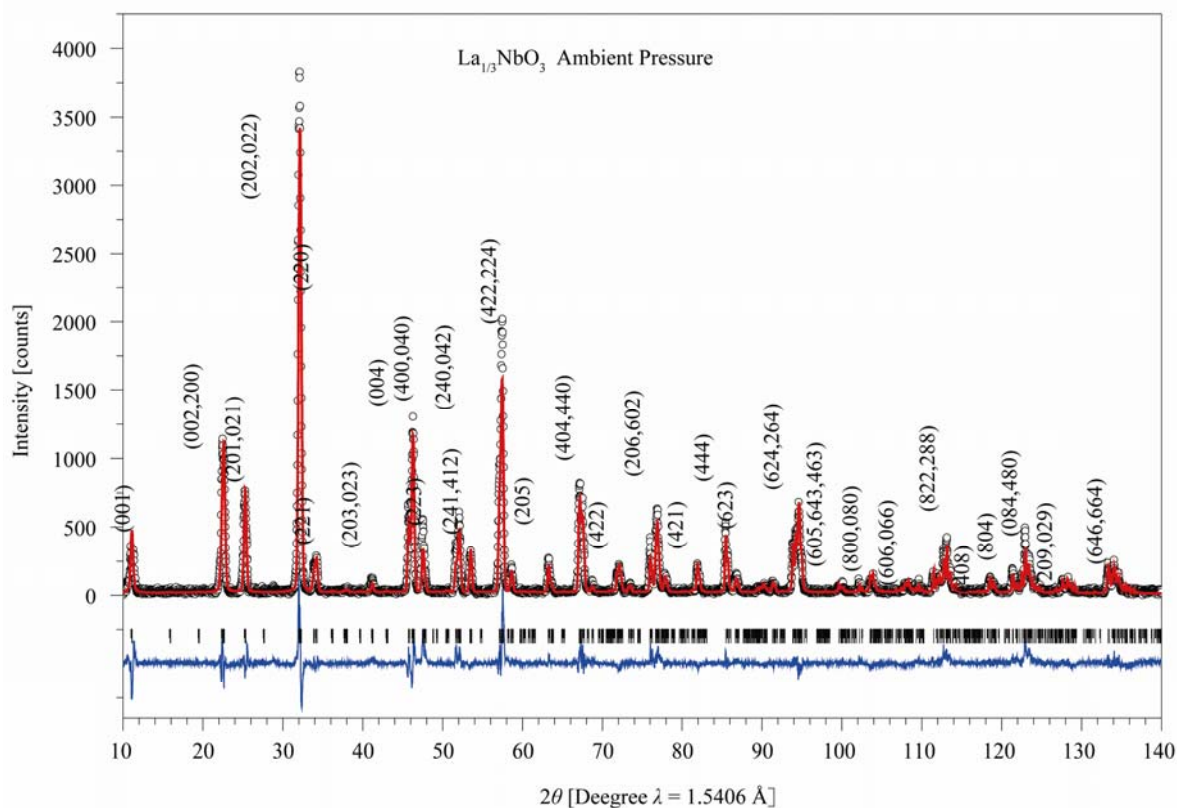


Figure 3. Rietveld analysis of the ADS spectrum of $\text{La}_{1/3}\text{NbO}_3$ at ambient pressure. The circles are the measured data and the red line is the Rietveld analysis to the Cmmm symmetry. The unit cell parameters are $a = 7.8422(2) \text{ \AA}$, $b = 7.8220(2) \text{ \AA}$ and $c = 7.9147(2) \text{ \AA}$. $R_{wp} = 4.190\%$, the blue line is the difference between the measured data and the fitting line. The vertical lines indicate the peak positions for the Cmmm symmetry. (NSLS - ADS 2010)

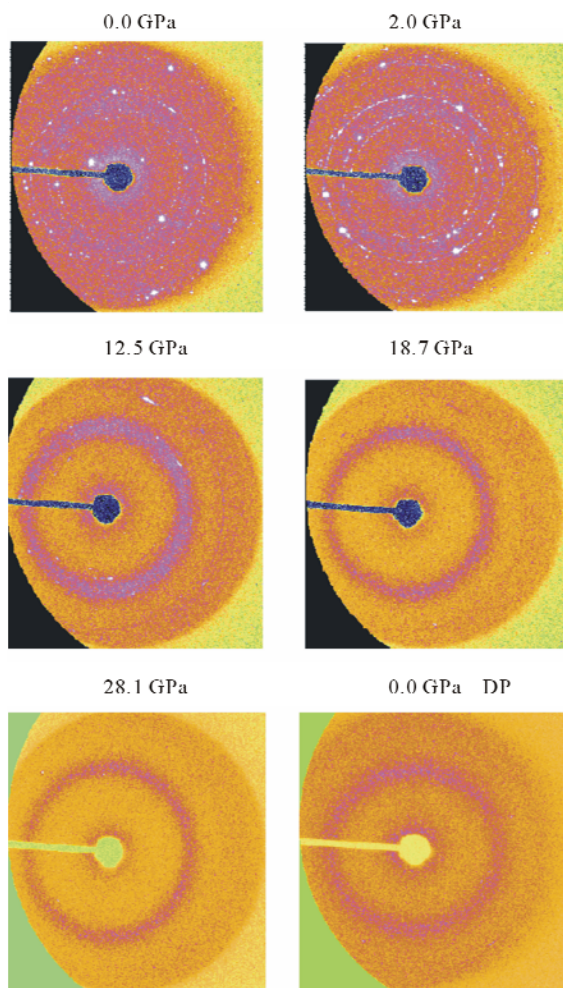


Figure 4. The ADS diffraction results as a function of high pressure. The sample is crystalline below ~ 10 GPa and amorphous above that pressure. The transition is not reversible upon releasing the pressure. (NLSL - $\lambda = 0.4066 \text{ \AA}$ - 2008)

crystallographic structure and the unit cell parameters as functions of pressure. The amorphous state was treated by analyzing the response of the first peak, first neighbors, to the external pressure. By releasing the high pressure we checked the irreversible amorphization of $\text{La}_{1/3}\text{NbO}_3$ under high-pressure.

3.1. Crystalline Phase

The $\text{La}_{1/3}\text{NbO}_3$ compound has a perovskite related structure, where the La atoms occupy dodecahedral sites and the Nb^{5+} ions are located in octahedral sites (see **Figure 6**). The original perovskite structure has 12 coordinated cavities, forming planes at $Z = 0$ and $Z = 1/2$. In our structure the $Z = 1/2$ sites are empty while $2/3$ of the $Z = 0$ sites are randomly occupied by the rare earth atoms.

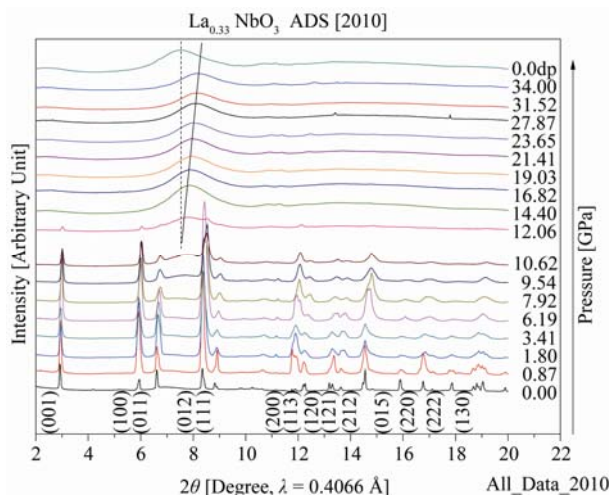


Figure 5. the ADS diffraction as function of pressure. The sample is crystalline below ~ 8 GPa and amorphous above ~ 12 GPa. Between these pressures, a superposition of crystalline and amorphous states exists. The transition is not reversible upon releasing the pressure. (NLSL - $\lambda = 0.4066 \text{ \AA}$ - 2010)

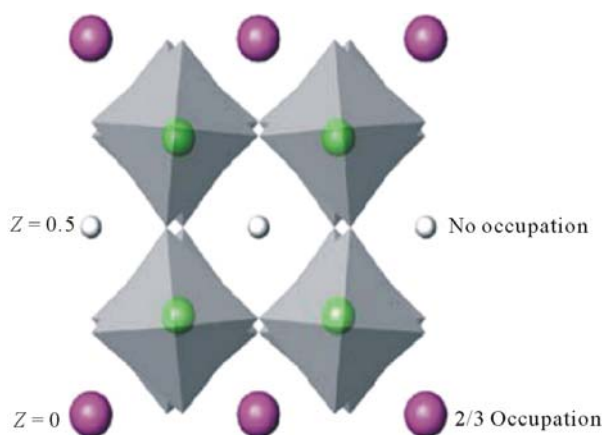


Figure 6. $\text{La}_{1/3}\text{NbO}_3$ supercell showing Nb cations at the octahedral centers [10].

Nb ions are displaced from the centers of the octahedra. The NbO_6 octahedra were found to be greatly distorted, thus making identification of the tilt system difficult. This cation-deficient perovskite structure has numerous vacant sites at $0, 0, 1/2$, which could easily accommodate a new ion. This has important consequences for the conductivity of the material.

The crystal structure and lattice parameters were extracted from the lower pressure ADS X-ray data. The crystalline phase is clearly identified in the pressure range of $0 - 10.6$ GPa while the two upper diffractions, 9.54 GPa and 10.62 GPa, have an amorphous part as well. The reduction in the unit cell volume in the crystalline region is of 5% at 10.62 GPa.

As we can see in **Figure 7**, the X-ray diffraction peaks are shifted to the higher 2θ values as the pressure increases, indicating the decreasing of the unit cell parameter as function of pressure.

The Rietveld analysis were based on the parameters that given in **Table 1**. We have assumed that the orthorhombic Cmmm (65) structure found by Kennedy [10] is maintained in $\text{La}_{1/3}\text{NbO}_3$.

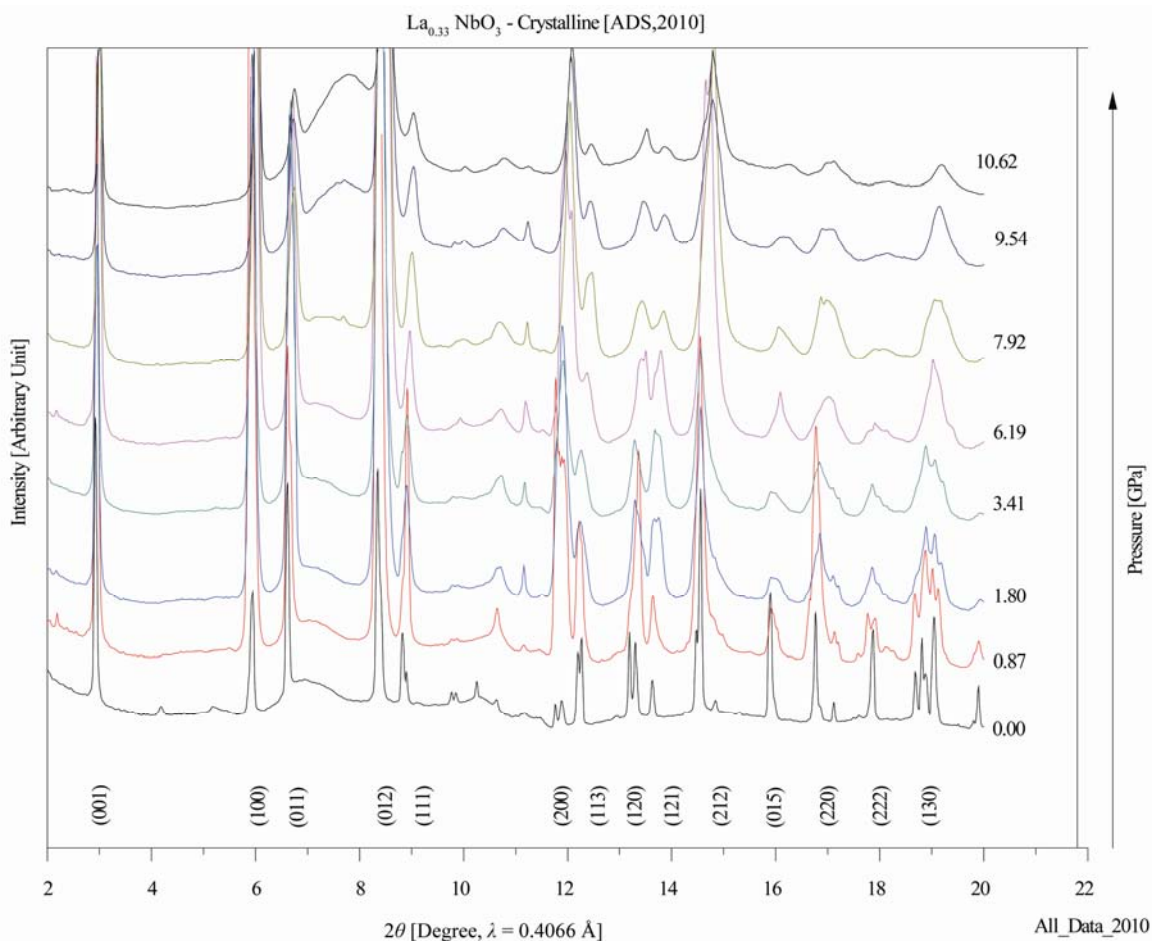


Figure 7. The low-pressure ADS diffraction patterns as a function of pressure. The sample is partially amorphous above 9.5 GPa. The transition is not reversible upon pressure release. The orthorhombic (Cmmm S.G. 65) symmetry is clearly present, in agreement with Kennedy [10]. (NLSL - ADS - 2010)

Table 1. $\text{La}_{1/3}\text{NbO}_3$: Crystallographic unit cell parameters.

Site	Wyck.	x/a	y/b	z/c	SOF	
La1	4g	0.2516	0	0	0.6667	1/3
La2	4h	0.2500	0	0.5000	0	0
Nb	8n	0	0.2616	0.2630	1	1
O 1	4i	0	0.2736	0	1	0.5
O 2	4j	0	0.2253	0.500	1	0.5
O 3	4k	0	0	0.2190	1	0.5
O 4	4l	0	0.5000	0.2577	1	0.5
O 5	8 m	0.2500	0.2500	0.2341	1	1

Orthorhombic Cmmm (65) $a = 7.8562 \text{ \AA}$, $b = 7.8361 \text{ \AA}$, $c = 7.9298 \text{ \AA}$.

An example of a Rietveld analysis performed on an ADS X-ray diffraction pattern from $\text{La}_{1/3}\text{NbO}_3$ at high pressure is given in **Figure 8**. In the Rietveld analysis, we are optimizing the diffraction spectrum by refining the unit cell parameters under the assumption of orthorhombic symmetry (Cmmm S.G.65). The initial atom positions and occupations were taken from Kennedy work [10].

Rietveld analysis of the ADS spectrum of $\text{La}_{1/3}\text{NbO}_3$ at 3.4 GPa is given in Fig 8. In that fitting the circles are the measured data and the red line is the fitted Rietveld analysis to the Cmmm symmetry. The unit cell parameters are $a = 7.844(6)$ Å, $b = 7.824(4)$ Å, $c = 7.904(6)$ Å. $R_{wp} = 4.190\%$, the blue gives the difference between the measured data and the fitting line. The vertical lines indicate the peak positions for the Cmmm symmetry with the fitted parameters.

The reduction of the unit cell parameters with increasing pressure is shown in **Figure 9**. The unit cell parameters were extracted from the Rietveld analysis.

The EOS (Equation of State) for the $\text{La}_{1/3}\text{NbO}_3$ was found by fitting the pressure to the reduction in the relative volume. The data was fitted to the Vinet equation [15].

$$P(v) = 3B_0 \left(\frac{v}{V_0} \right)^{\frac{2}{3}} \left(1 - \left(\frac{v}{V_0} \right)^{\frac{1}{3}} \right) \exp \left(\frac{2}{3} (B'_0 - 1) \left(1 - \left(\frac{v}{V_0} \right)^{\frac{1}{3}} \right) \right) \quad (1)$$

where B_0 is the isothermal bulk modulus at room temperature and ambient pressure, and B'_0 is the partial derivative of the isothermal bulk modulus against pressure under the same conditions. The B_0 parameter for the monoclinic phase symmetry is (183.0 ± 9.9) GPa, with a fixed B'_0 as 4. We can see in **Figure 10** that the data fits to the measurement of 2008 and 2010 as well.

3.2. Amorphous Phase

The EDS (Energy dispersive system) was measured at beamline X17C of the NSLS by introducing a white beam from the super-conducting wiggler. We measured the X-ray diffraction at three different angles (8° , 10° and 12°).

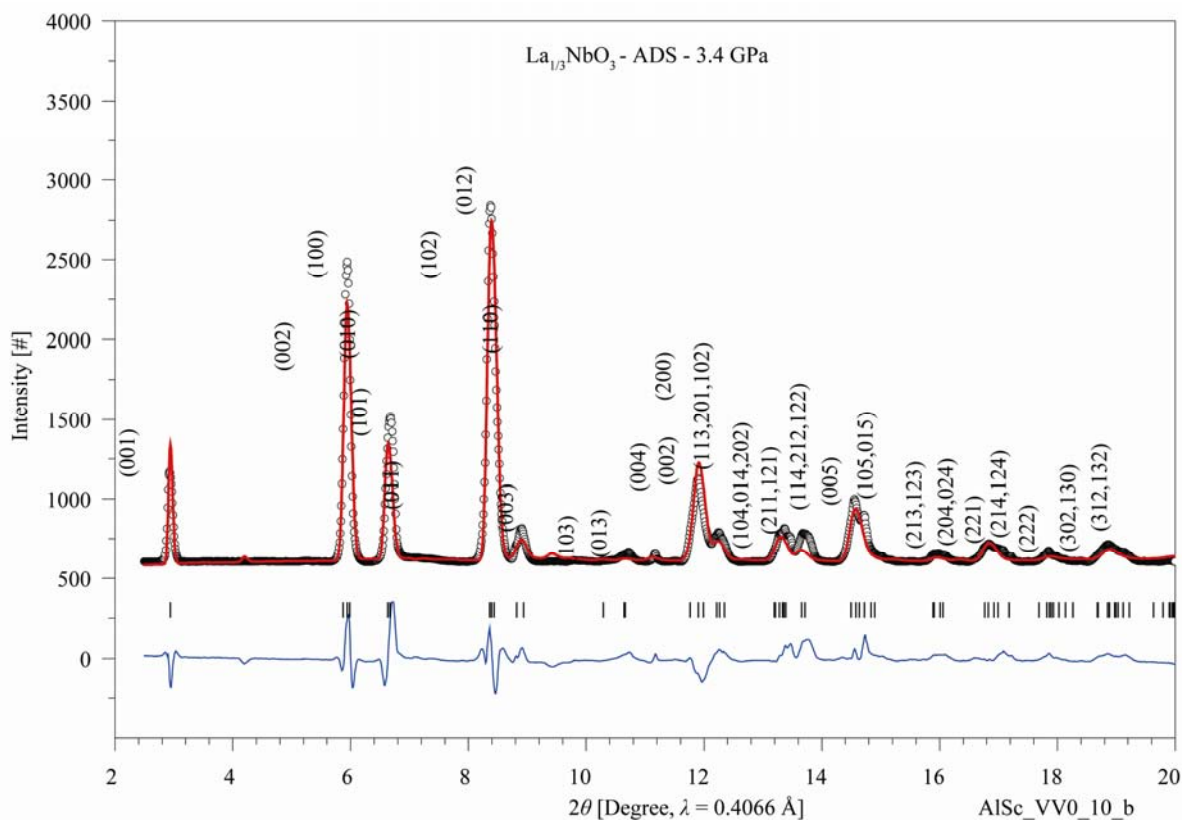


Figure 8. Rietveld analysis of the ADS spectrum of $\text{La}_{1/3}\text{NbO}_3$ at 3.4 GPa. The circles are the measured data and the red line is the Rietveld analysis to the Cmmm symmetry. The unit cell parameters are $a = 7.844(6)$ Å, $b = 7.824(4)$ Å, $c = 7.904(6)$ Å. $R_{wp} = 4.190\%$ and $GOF = 5.59\%$. The blue line is the difference between the measured data and the fitting line. The vertical lines indicate the peak positions for the Cmmm symmetry. (NSLS - ADS 2010)

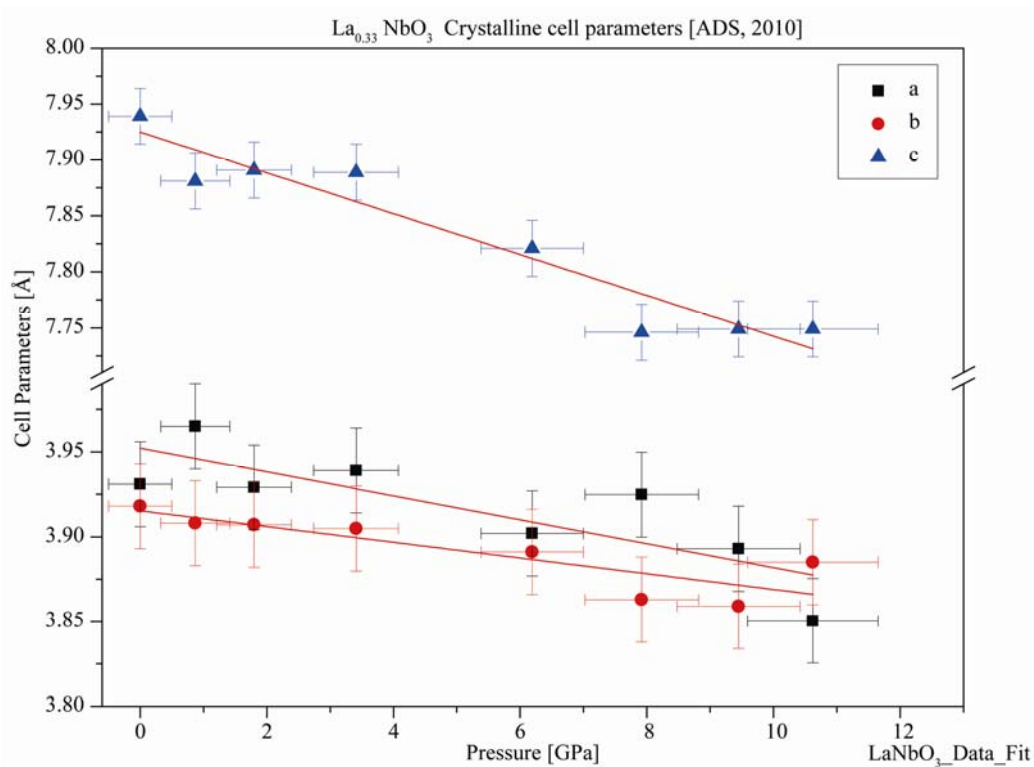


Figure 9. The unit cell parameters from the Rietveld analysis of the ADS spectrum of $\text{La}_{1/3}\text{NbO}_3$ in the pressure range of 0 - 10.62 GPa. The red line is a guiding line that indicates the reduction in the unit cell parameter as a function of pressure. (NSLS ADS 2010).

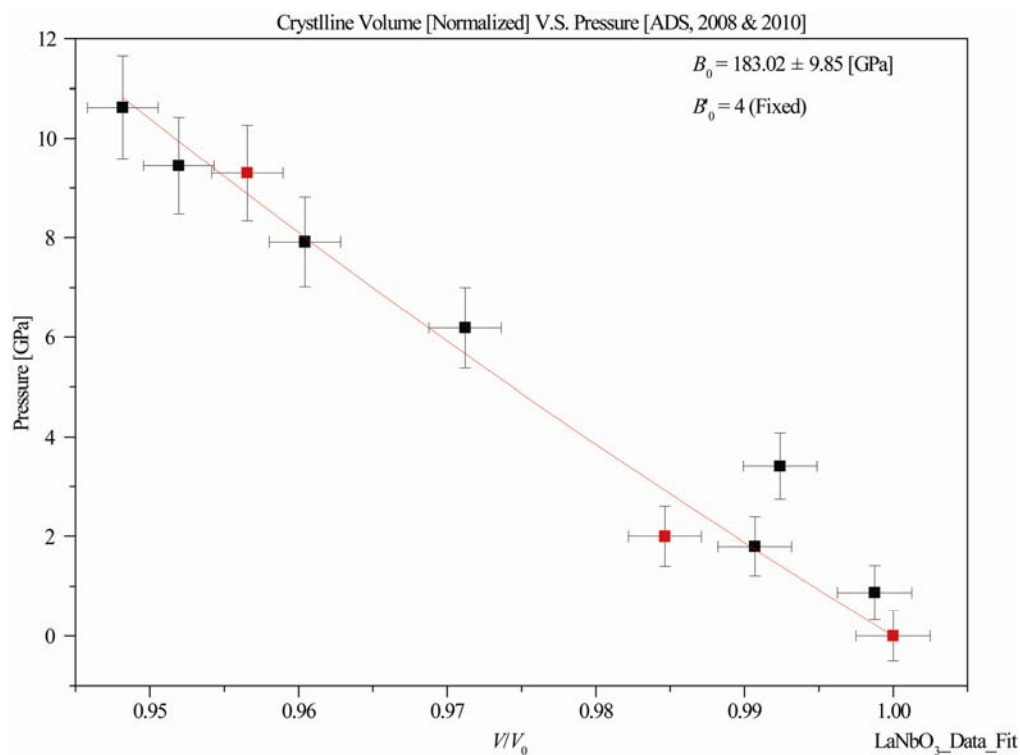


Figure 10. The relative volume change as a function of high pressure in the crystalline region. The volumes are derived from the unit cell parameters from the Rietveld analysis of the ADS. (NSLS - ADS 2008, 2010)

Each measurement lasted 20 minutes. A HPGe detector was used. In the spectrum we can see the fluorescent lines of the constituents of the sample. In this set we clearly see that the $\text{La}_{1/3}\text{NbO}_3$ is in an amorphous state and that this state is not reverse while decreasing the pressure. An example of the EDS X-ray diffraction at an angle of 8° is depicted in **Figure 11**.

This data is hard to interpret and we use it only to establish that we have an irreversible amorphization of $\text{La}_{1/3}\text{NbO}_3$ under high-pressure.

We measured the ADS X-ray diffraction pattern of the $\text{La}_{1/3}\text{NbO}_3$ sample at high pressure in 2008 and again in 2010. This is shown in **Figure 12**. We can clearly identify an amorphous state above 12.5 GPa in 2008 and above 9.5 GPa in 2010. In both spectrums, we find non reversibility in the amorphous state upon lowering the pressure.

We analyzed the reduction in the unit cell parameters by measuring the first atom neighbor peak near 7° .

$$\left[\frac{v}{V_{p=0}} \right]^{1/3} = \frac{d}{d_{p=0}} \approx \frac{Q_{p=0}}{Q} \quad d \approx \frac{2\pi}{Q} \quad (2)$$

The EOS (Equation of State) for the $\text{La}_{1/3}\text{NbO}_3$ in the amorphous state was found by fitting the pressure to the reduction in the relative volume. The data was fitted to the Vinet equation [15].

We used the form of the Vinet equation in which the initial Volume, V_0 , is a fitted parameter. From the fitting data we get $V_0 = (29.15 \pm 0.05) \text{ \AA}^3$, $B_0 = (84.89 \pm 1.17) \text{ GPa}$ and $B'_0 = 4$ (fixed), see **Figure 13**.

In **Figure 14** the EOS is summarized for the crystallized and the amorphous states. In the crystallized region the unit cell volume lose 5% of its magnitude and in the amorphous region a further 11.3% decrease occurs.

The bulk modulus differs much between the crystalline and amorphous phase. (NSLS - ADS 2008, 2010)

4. Conclusions

The $\text{La}_{1/3}\text{NbO}_3$ crystallize in the orthorhombic, Cmmm Space Group 65. The Crystallographic parameters at ambient pressure are $a = 7.8562 \text{ \AA}$, $b = 7.8361 \text{ \AA}$, and $c = 7.9298 \text{ \AA}$. In the range of pressure from 0 - ~ 10 GPa the

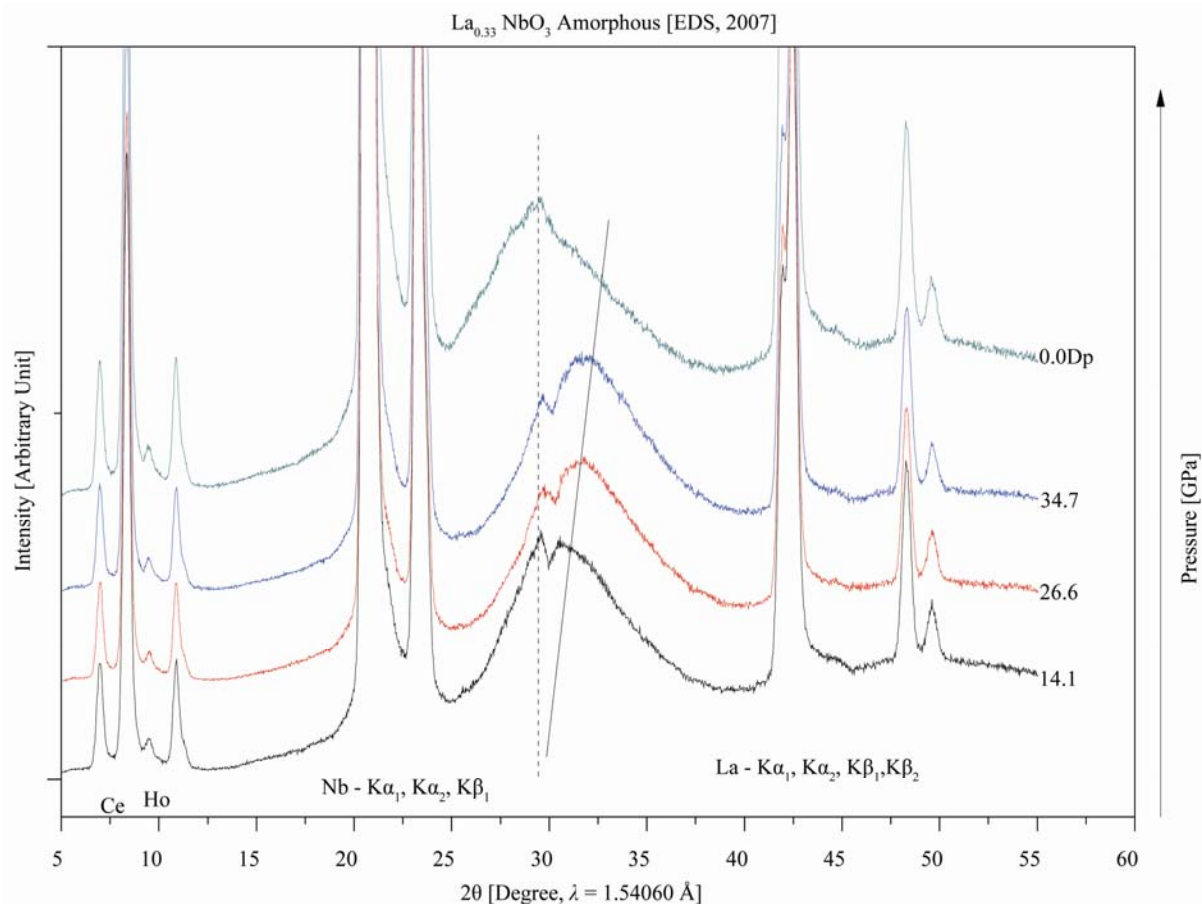


Figure 11. The EDS diffraction as function of high pressure. The sample is amorphous above 14 GPa. The transition is not reversible when the pressure is released. (NSLS - EDS 2007)

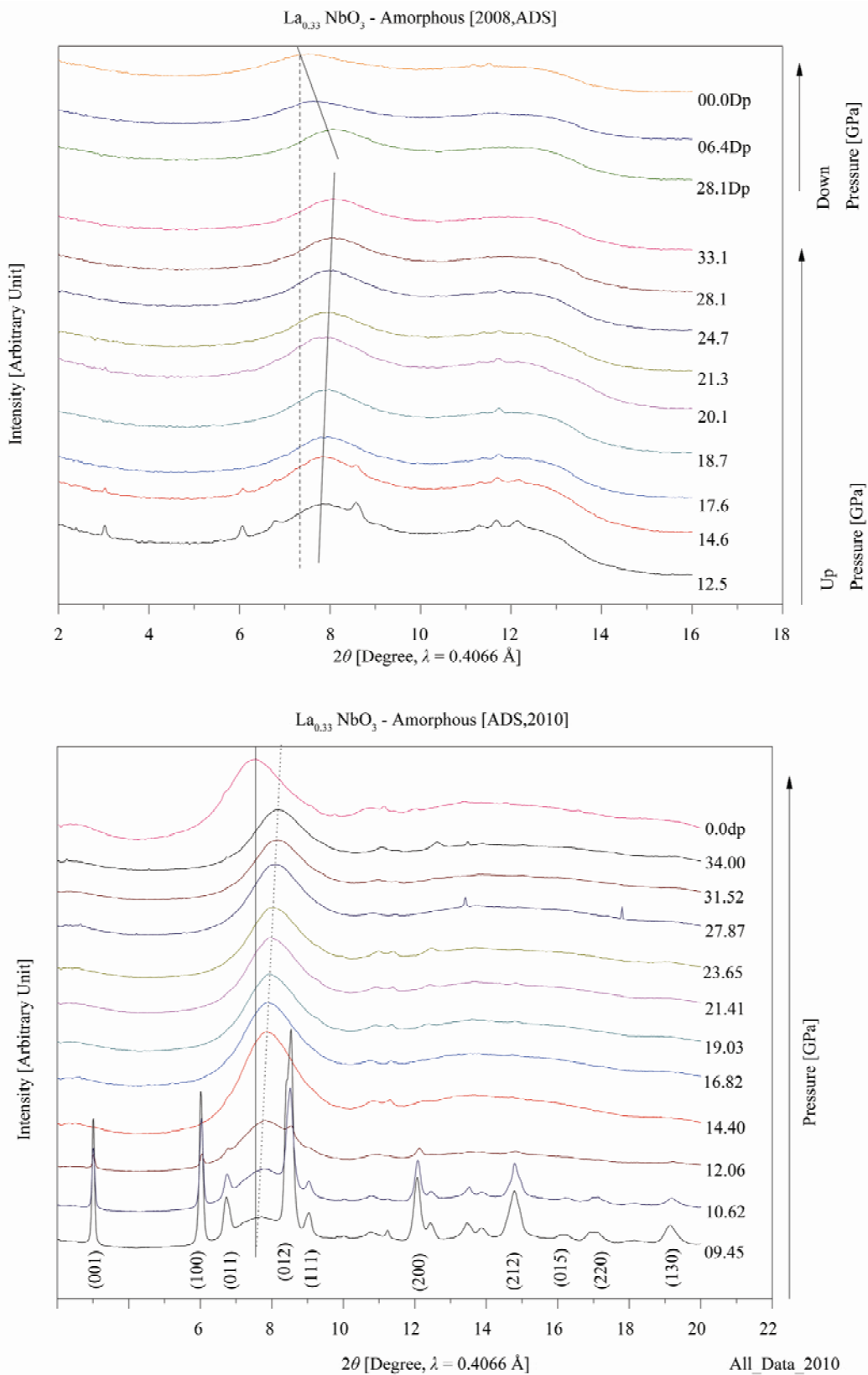


Figure 12. The ADS diffraction as function of high pressure. The sample is partially amorphous above 9.5 GPa. The transition is not reversible. (NSLS - ADS 2008, 2010)

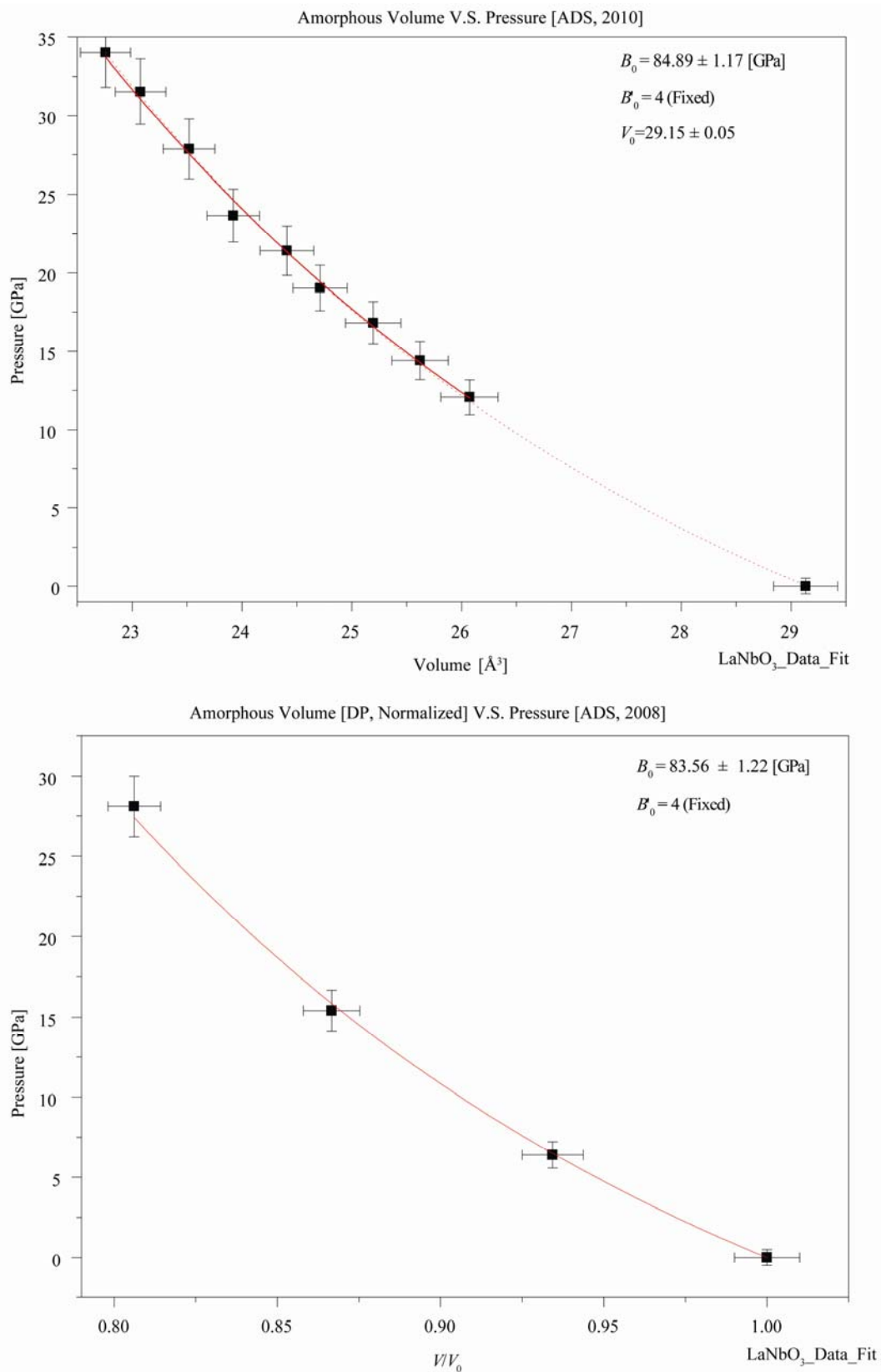


Figure 13. The ADS diffraction as function of high pressure. The sample is amorphous above ~12 GPa. The transition is not reversible. (NSLS - ADS 2008, 2010)

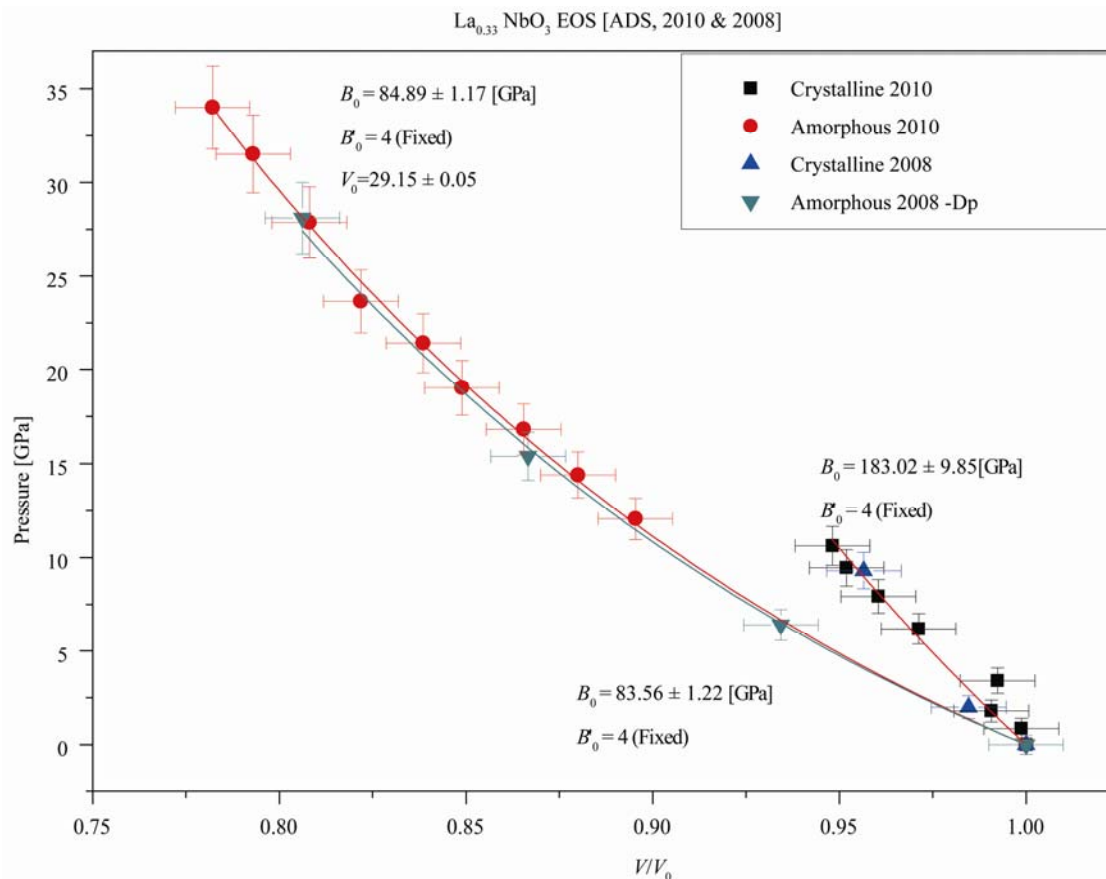


Figure 14. The EOS of La_{1/3}NbO₃ for the crystalline and amorphous phase.

La_{1/3}NbO₃ keeps the orthorhombic structure. There is a range of ~2 GPa above the orthorhombic structure in which a crystalline and amorphous state coexist.

The EOS (Equation of State) for the La_{1/3}NbO₃ in the crystalline state yields a B_0 of (183.03 ± 9.85) GPa (with a B'_0 fixed to 4.0). The unit cell volume of La_{1/3}NbO₃ is reduced by 5% under pressure in the crystalline state region. Above 12 GPa the La_{1/3}NbO₃ amorphous state is maintained up to the maximum pressure reached in this study.

The EOS (Equation of State) for the La_{1/3}NbO₃ in the amorphous state was found by fitting the pressure to the reduction in the relative volume. The data was fitted to the Vinet equation.

The Vinet equation yielded $V_0 = (29.15 \pm 0.05) \text{ \AA}^3$, $B_0 = (84.89 \pm 1.17)$ GPa and $B'_0 = 4$ (fixed). The amorphous phase is apparently much softer than the crystalline phase. The EOS for both the crystallized and the amorphous state is summarized in the **Figure 14**. It is clear that there is a softening above ~12 GPa. In the crystallized region the unit cell volume loses of 5% and in the amorphous region a further 11.3% is lost.

In conclusion, we clearly find an irreversible, pressure-induced amorphization of La_{1/3}NbO₃.

5. Acknowledgements

We wish to thank Dr. M. Avdeev from the *Bragg Institute, Australian Nuclear Science and Technology Organisation*, for preparing the La_{1/3}NbO₃ sample and for performing the chemical analysis.

6. References

- [1] Y. Inaguma, L. Chen, M. Itoh, T. Nakamura, T. Uchida, H. Ikuta and M. Wakihara, "High Ionic Conductivity in Lithium Lanthanum Titanate," *Solid State Communications*, Vol. 86, No. 10, 1993, pp. 689-693. doi:10.1016/0038-1098(93)90841-A
- [2] G. X. Wang, P. Yao, D. H. Bradhurst, S. X. Dou and H. K. Liu, "Structure Characterisation and Lithium Insertion in La_{0.33}NbO₃ Perovskite," *Solid State Ionics*, Vol. 124, No. 1-2, 1999, pp. 37-43. doi:10.1016/S0167-2738(99)00138-1
- [3] W. J. Merz, "The Electric and Optical Behavior of BaTiO₃ Single-Domain Crystals," *Physical Review*, Vol. 76, No. 8, 1949, pp. 1221-1225. doi:10.1103/PhysRev.76.1221
- [4] A. P. Ramirez, R. J. Cava and J. Krajewski, "Colossal Magnetoresistance in Cr-Based Chalcogenide Spinels," *Nature*, Vol. 386, No. 6621, 1997, pp. 156-159.

- doi:10.1038/386156a0
- [5] O. Bohnke, J. Emery, A. Veron, J. L. Fourqueta, J. Y. Buzareb, P. Florianc and D. Massiotc, "A Distribution of Activation Energies for the Local and Long-Range Ionic Motion is Consistent with the Disordered Structure of the Perovskite $\text{Li}_{3x}\text{La}_{2/3-x}\text{TiO}_3$," *Solid State Ionics*, Vol. 109, No. 1-2, 1998, pp. 25-34.
doi:10.1016/S0167-2738(98)00081-2
- [6] Y. Harada, T. Ishigaki, H. Kawai and J. Kuwano, "Lithium Ion Conductivity of Polycrystalline Perovskite $\text{La}_{0.67-x}\text{Li}_{3x}\text{TiO}_3$ with Ordered and Disordered Arrangements of the A-Site Ions," *Solid State Ionics*, Vol. 108, No. 1-4, 1998, pp. 407-413.
doi:10.1016/S0167-2738(98)00070-8
- [7] Y. Shan, N. Sinozaki and T. Nakamura, "Preparation and Characterizations of New Perovskite Oxides ($\text{La}_x\text{Na}_{1-3x-y}\text{Li}_{y-2x}$) NbO_3 ($0.0 \leq x$ and $y \leq 0.2$)," *Solid State Ionics*, Vol. 108, No. 1-4, 1998, pp. 403-406.
doi:10.1016/S0167-2738(98)00069-1
- [8] Y. Kawakami, M. Fukuda, H. Ikata and M. Wakihara, "Ionic Conduction of Lithium for Perovskite Type Compounds, ($\text{Li}_{0.05}\text{La}_{0.317}$) $_{1-x}\text{Sr}_{0.5x}\text{NbO}_3$, ($\text{Li}_{0.1}\text{La}_{0.3}$) $_{1-x}\text{Sr}_{0.5x}\text{NbO}_3$ and ($\text{Li}_{0.25}\text{La}_{0.25}$) $_{1-x}\text{M}_{0.5x}\text{NbO}_3$ (M = Ca and Sr)," *Solid State Ionics*, Vol. 110, No. 3-4, 1998, pp. 187-192.
doi:10.1016/S0167-2738(98)00131-3
- [9] C. Bohnke, O. Bohnke and J. L. Fourquet, "Electrochemical Intercalation of Lithium into $\text{LiLaNb}_2\text{O}_7$ Perovskite," *Journal of the Electrochemical Society*, Vol. 144, No. 4, 1997, pp. 1151-1158. doi:10.1149/1.1837565
- [10] B. J. Kennedy, C. J. Howard, Y. Kubota and K. Kato, "Phase Transition Behaviour in the A-Site Deficient Perovskite Oxide $\text{La}_{1/3}\text{NbO}_3$," *Journal of Solid State Chemistry*, Vol. 177, No. 12, 2004, pp. 4552-4556.
doi:10.1016/j.jssc.2004.08.047
- [11] E. Sterer, M. P. Pasternak and R. D. Taylor, "A Multi-purpose Miniature Diamond Anvil Cell," *Review of Scientific Instruments*, Vol. 61, No. 3, 1990, pp. 1117-1119.
doi:10.1063/1.1141433
- [12] R. A. Forman, G. J. Piermarini, J. D. Barnett and S. Block, "Pressure Measurement Made by the Utilization of Ruby Sharp-Line Luminescence," *Science*, Vol. 176, No. 4032, 1972, pp. 284-285.
doi:10.1126/science.176.4032.284
- [13] H. M. Rietveld, "A Profile Refinement Method for Nuclear and Magnetic Structures," *Journal of Applied Crystallography*, Vol. 2, 1969, pp. 65-71.
doi:10.1107/S0021889869006558
- [14] A. Hammersley, Program Fit2D (Version: V12.077), ESRF 2009.
- [15] P. Vinet, J. Ferrante, J. H. Rose and J. R. Smith, "Compressibility of Solids," *Journal of Geophysical Research*, Vol. 92, No. B9, 1987, pp. 9319-9325.
doi:10.1029/JB092iB09p09319